F2012-D05-001

GPS BASED ESTIMATION OF VEHICLE SIDESLIP ANGLE USING MULTI-RATE KALMAN FILTER WITH PREDICTION OF COURSE ANGLE MEASUREMENT RESIDUAL

[1]Nguyen, Binh Minh[*]; [2]Wang, Yafei; [2]Oh, Sehoon; [1]Fujimoto, Hiroshi; [1]Hori, Yoichi
[1]Department of Advanced Energy, the University of Tokyo, Japan;
[2]Department of Electrical Engineering, the University of Tokyo, Japan

KEYWORDS – sideslip angle, GPS, multi-rate, Kalman filter, measurement residual

ABSTRACT – In this paper, a new vehicle sideslip angle estimation based on GPS is proposed. Course angle obtained from GPS receiver can be utilized as one measurement for estimation design, and the other measurement is yaw rate from gyroscope. While yaw rate is sampled every 1 millisecond, due to the limitation of GPS receiver the sampling time of course angle is much longer (200 millisecond). During inter-samples (between two updates of course angle), the conventional estimation method relies upon only yaw rate measurement. In order to enhance the estimation accuracy, multi-rate Kalman filter with the prediction of course angle measurement residual during inter-samples is designed. Experiments are conducted to verify the effectiveness of the proposed algorithm.

INTRODUCTION

Sideslip angle estimation technique plays an important role in vehicle stability control (VSC). In VSC system, sideslip angle must be controlled to prevent the vehicle accidents which may happen in critical driving situations, such as vehicle cornering into slippery road at high speed [1]. In fact, current vehicles are not equipped with an ability of measuring sideslip angle directly. Corrsys-Datron provides the noncontact optical sensor for sideslip angle calculation based on lateral and longitudinal velocity measurement [2]. Because of its high cost, Corrsys-Datron sensor cannot be a practical solution. For both cost reducing and safety purpose, sideslip angle estimation has been a big issue in motion control of vehicle.

In conventional sideslip angle estimation method, lateral accelerometer is used as output measurement [3]. Therefore, cornering stiffness appears in the measurement equations. In fact, the variation of road friction introduces uncertainties into the estimation model. In order to improve the sideslip angle estimation, non-conventional sensors have been utilized, such as visual information using camera image processing [4], attitude information from GPS receiver [5], [6], and the measurement of tire lateral force sensor [7]. However, the poor update rate of image processing is the main disadvantage of this approach. Camera visibility may also be unavailable when road makers are covered with leaves, snow, water, or dirt. Like visual based estimation, the main problem of GPS based estimation is the update rate of GPS receiver (from 1 to 10 Hz) which is not fast enough for motion control of vehicle. The high cost of tire force sensors is a question for the application of this method in commercial vehicles.

Thanks to Japan's own GPS system which has been constructed as national projects, high accuracy of vehicle motion measurement based on GPS is achieved. In this paper, sideslip angle estimation based on multi-rate Kalman filter is designed using yaw rate (sampling time of 1 millisecond) and course angle obtained from GPS receiver (sampling time of 200 millisecond in this study). Using course angle measurement, cornering stiffness disappears in

the measurement equations. The estimation steps between two continuous updates of course angle is called inter-samples in this paper. During inter-samples, conventional multi-rate Kalman filter relies upon yaw rate measurement only. In this study, prediction of course angle measurement residual during inter-samples is proposed. Therefore, sideslip angle is estimated every 1 millisecond with high accuracy, even under model uncertainties, such as the variation of cornering stiffness.

The proposed method is implemented in the control system of in-wheel motored electric vehicle COMS prototyped by Toyota Auto Body Co., Ltd. Two in-wheel motors are equipped in the rear wheels to generate the yaw moment. A RT-Linux operating system computer is used as the controller of COMS with the control period of 1 millisecond. A Corrsys-Datron optical sensor installed in the front of vehicle can be used to calculate the sideslip angle at the center of gravity. GPS receiver CCA-600 is supported by Japan Radio Co., Ltd. It can provide the measurement of vehicle course angle with the accuracy of 0.14 degree RMS every 200 millisecond. This is more accurate than the one used at Stanford University (course angle accuracy of 0.25 degree RMS) for the research in [5]. Experimental vehicle and GPS receiver are shown in Fig. 1.

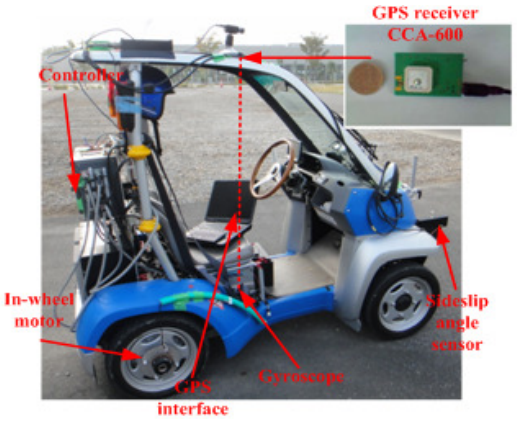

Fig. 1. Electric vehicle COMS.

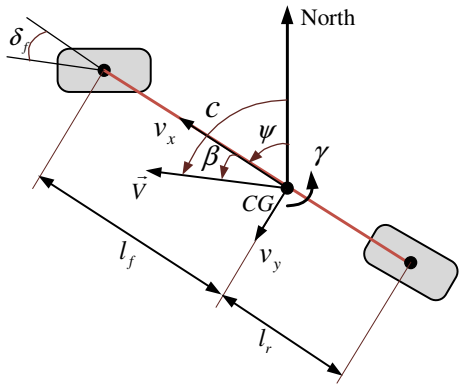

Fig. 2. Planar bicycle model of vehicle.

TABLE 1
NOMENCLATURES

l_f, l_r	Distances from front (rear) axle to the center of gravity
C_f, C_r	Front (rear) cornering stiffness
I_z	Yaw moment of inertia
δ_f	Front steering angle
N_z	Yaw moment generated by in-wheel motors
M	Vehicle mass
β	Sideslip angle
γ	Yaw rate
ψ	Yaw angle
c	Course angle obtained from GPS
v_x, v_y, V	Longitudinal, lateral, and velocity vector

MODELING OF VEHICLE DYNAMICS

The planar bicycle model of vehicle is shown in Fig. 2. This model is constructed under the following assumptions: 1) Tire slip angle is small such that lateral tire force is at linear region. 2) Vehicle is symmetric about the fore-and-aft center line. 3) Load transfer is neglected. 4) Vehicle velocity is approximately constant. Table 1 shows the list of nomenclatures. Sideslip angle is defined as the angle between velocity vector and longitudinal direction. Course angle of a moving vehicle is the angle between vehicle's direction and geodetic North. Using this definition, course angle can be represented as the summary of yaw angle and sideslip angle:

$$c = \psi + \beta \tag{1}$$

The lateral force equation and yaw moment equation can be expressed as follows:

$$F_{yf} + F_{yr} = Mv_x\left(\dot{\beta} + \gamma\right) \tag{2}$$

$$F_{yf} l_f - F_{yr} l_r + N_z = I_z \dot{\gamma} \tag{3}$$

Where

$$F_{yf} = -2C_f \alpha_f = -2C_f\left(\delta_f - \frac{l_f}{v_x}\gamma - \beta\right) \tag{4}$$

$$F_{yr} = -2C_r \alpha_r = -2C_r\left(\frac{l_r}{v_x}\gamma - \beta\right) \tag{5}$$

From (1)-(5), the state space equation of vehicle dynamics is constructed as (6)-(10). Front steering angle and yaw moment are selected as input vector.

$$\dot{x} = Ax + Bu \tag{6}$$

$$x = \begin{bmatrix}\beta & \gamma & \psi\end{bmatrix}^T \tag{7}$$

$$u = \begin{bmatrix}\delta_f & N_z\end{bmatrix}^T \tag{8}$$

$$A = \begin{bmatrix} \dfrac{-2\left(C_f + C_r\right)}{Mv_x} & -1 - \dfrac{2\left(C_f l_f - C_r l_r\right)}{Mv_x^2} & 0 \\ \dfrac{-2\left(C_f l_f - C_r l_r\right)}{I_z} & \dfrac{-2\left(C_f l_f^2 + C_r l_r^2\right)}{I_z v_x} & 0 \\ 0 & 1 & 0 \end{bmatrix} \tag{9}$$

$$B = \begin{bmatrix} \dfrac{2C_f}{Mv_x} & 0 \\ \dfrac{2C_f l_f}{I_z} & \dfrac{1}{I_z} \\ 0 & 0 \end{bmatrix} \tag{10}$$

PREDICTION OF INTER-SAMPLE MEASUREMENT RESIDUALS

Dynamics of Single-rate Kalman Filter

For the sake of simplicity, steady state Kalman filter is used to derive the dynamics of measurement residual. Assume that the output measurement's sampling time is the same as the control period T_c. The discrete model under process noise w_{k-1} and measurement noise v_k is expressed as follows:

$$\begin{cases} x_k = A_d x_{k-1} + B_d u_{k-1} + w_{k-1} \\ y_k = C_d x_k + v_k \end{cases} \tag{11}$$

The Kalman filter has two stages as follows where L_d is the Kalman gain matrix.

- Prediction:

$$\overline{x}_k = A_d \hat{x}_{k-1} + B_d u_{k-1} \tag{12}$$

- Correction:

$$\hat{x}_k = \overline{x}_k + L_d \varepsilon_k = \overline{x}_k + L_d \left(y_k - C_d \overline{x}_k \right) \tag{13}$$

Where ε_k is the measurement residual which is updated every T_c in this case. From (11)-(13), the measurement residual is derived as follows:

$$\varepsilon_k = C_d A_d e_{k-1} + C_d w_{k-1} + v_k \tag{14}$$

From (11)-(14), the dynamics of estimation error is obtained as:

$$e_k = \left(I - L_d C_d \right) A_d e_{k-1} + \left(I - L_d C_d \right) w_{k-1} - L_d v_k \tag{15}$$

The measurement residual in the next estimation step can be derived as:

$$\varepsilon_{k+1} = C_d A_d e_k + C_d w_k + v_{k+1} \tag{16}$$

From (15) and (16), under zero-noise condition, the relation between measurement residual at step $k+1$ and measurement residual at step k is derived as:

$$\varepsilon_{k+1} = Q_d \varepsilon_k = C_d A_d \left(I - L_d C_d \right) C_d^T \left(C_d C_d^T \right)^{-1} \varepsilon_k \tag{17}$$

The estimation error in the next n step can be derived as:

$$e_{k+n} = \left[\left(I - L_d C_d \right) A_d \right]^{n+1} e_{k-1} + W_{sr,n} \left(w_{k-1}, w_k, ... w_{k+n-1} \right) + V_{sr,n} \left(v_k, v_{k+1}, ..., v_{k+n} \right) \tag{18}$$

$$W_{sr,n} \left(w_{k-1}, w_k, ... w_{k+n-1} \right) = \sum_{i=0}^{i=n} \left[\left(I - L_d C_d \right) A_d \right]^{n-i} \left(I - L_d C_d \right) w_{k-1+i} \tag{19}$$

$$V_{sr,n} \left(v_k, v_{k+1}, ..., v_{k+n} \right) = -\sum_{i=0}^{i=n} \left[\left(I - L_d C_d \right) A_d \right]^{n-i} L_d v_{k+i} \tag{20}$$

Dynamics of Conventional Multi-rate Kalman Filter

Assume that the measurement output's sampling time T_s is longer than the control period T_c. Define $r = T_s/T_c$ is the multi-rate ratio and it is assumed that r is an integer. The steps between two measurement update are named inter-samples. The dual-rate system is shown in Fig. 3. If measurement output is updated (at step $k = jr$), the prediction and estimation equation are the same as the single-rate case.

During inter-samples (at step $k+n$, $k = jr$, $n \in [1, r-1]$), because no new measurement is updated, the correction term $L_d \varepsilon_k$ is not accounted in the correction stage. Dynamics of estimation error during inter-samples is derived as follows:

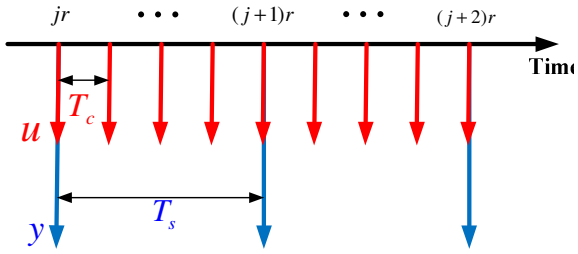

Fig. 3. Dual-rate system.

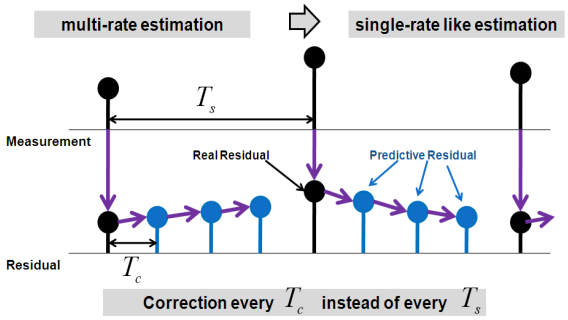

Fig. 4. Idea of inter-sample residual prediction.

$$e_{k+n} = A_d^n \left[\left(I - L_d C_d \right) A_d \right] e_{k-1} + W_{mr,n} \left(w_{k-1}, w_k, \ldots w_{k+n-1} \right) + V_{mr,n} \left(v_k \right) \tag{21}$$

$$W_{mr,n} \left(w_{k-1}, w_k, \ldots w_{k+n-1} \right) = A_d^n \left(I - L_d C_d \right) w_{k-1} + \sum_{i=0}^{i=n-1} A_d^{n-i-1} w_{k+i} \tag{22}$$

$$V_{mr,n} \left(v_k \right) = -A_d^n L_d v_k \tag{23}$$

Equation (21) shows that under model uncertainties with the influence of noises and disturbances, estimation performance may be degraded due to the lost of correction term $L_d \varepsilon_k$. The situation will be very serious if matrix A_d has unstable poles.

Proposal of Inter-sample Measurement Residual Prediction

The key idea can be explained using Fig. 4. If the measurement update is available, the real measurement residual is used to correct the estimated state. During inter-samples, the predictive measurement residuals are utilized to enhance the dynamics of the multi-rate estimation. The formulation of predictive residual is proposed as follows:

$$\tilde{\varepsilon}_{k+n} = Q_d^n \varepsilon_k, \quad k = jr, \; n \in [1, r-1] \tag{24}$$

By applying (24) for r -1 times, we can prove the general formulation of estimation error with prediction of inter-samples:

$$e_{k+n} = \left[\left(I - L_d C_d \right) A_d \right]^{n+1} e_{k-1} + W_{ehmr,n} \left(w_{k-1}, w_k, \ldots w_{k+n-1} \right) + V_{ehmr,n} \left(v_k \right) \tag{25}$$

$$W_{ehmr,n} \left(w_{k-1}, w_k, \ldots w_{k+n-1} \right) = \sum_{i=0}^{n} A_d^{n-i} w_{k-1+i} - \left(\sum_{i=0}^{n} A_d^{n-i} L_d Q_d^i \right) w_{k-1} \tag{26}$$

$$V_{ehmr,n} \left(v_k \right) = -\left(\sum_{i=0}^{n} A_d^{n-i} L_d Q_d^i \right) v_k \tag{27}$$

From (25), the dynamics of estimation error during inter-samples is improved in comparison with the case of conventional multi-rate as expressed in (21). However, the accuracy of inter-samples relies upon the past measurement at step $k = jr$. In case of single-rate estimation, as represented in (18), estimation error at any step is driven by the current and the past measurement noise. Thus, if the system is zero-noise, the proposed method has the same estimation error dynamics as the single-rate estimation. If a measurement error happens at step $k = jr$, the proposed estimation cannot be as good as the single-rate case. This is because the error at step $k = jr$ is transferred to every step during inter-samples. Even though, dynamics of estimation error of the proposed method is better than the conventional multi-rate estimation.

SIDESLIP ANGLE ESTIMATION DESIGN

Output Measurements

Yaw rate and course angle are selected as output measurements for Kalman filter design. The sampling time of yaw rate is the same as the control period T_c = 1 millisecond. Course angle is obtained from GPS receiver every T_s = 200 millisecond. Inter-samples are defined as the estimation steps between two continuous updates of course angle. The measurement equation is constructed as follows:

$$y_k = C_d x_k + v_k \tag{28}$$

Where the measurement matrix is:

$$C_d = \begin{bmatrix} 0 & 1 & 0 \\ 1 & 0 & 1 \end{bmatrix} \tag{29}$$

Discrete Model

The continuous model in (6) is transformed into discrete model (30) by using the transformation (31) and (32). T_c = 1 millisecond is the fundamental sampling time.

$$x_k = A_d x_{k-1} + B_d u_{k-1} + w_{k-1} \tag{30}$$

$$A_d = e^{AT_c} \approx A\left(T_c I\right) + I \tag{31}$$

$$B_d = \int_0^{T_c} e^{A\tau} d\tau B \approx B\left(T_c I\right) \tag{32}$$

Multi-rate Kalman Filter Algorithm

Kalman filter is designed based on the dynamics model (29) and the measurement equation (27). Q_v and Q_w are the process noise and measurement noise covariance matrices, as expressed in (32) and (33), respectively. They are tuning parameters of the Kalman filter algorithm shown in Fig. 5.

$$Q_v = \begin{bmatrix} \sigma^2_{\gamma\_gyro} & 0 \\ 0 & \sigma^2_{c\_GPS} \end{bmatrix} \tag{33}$$

$$Q_w = \begin{bmatrix} q_{11}^2 & 0 & 0 & 0 & 0 \\ 0 & q_{22}^2 & 0 & 0 & 0 \\ 0 & 0 & q_{33}^2 & 0 & 0 \\ 0 & 0 & 0 & q_{44}^2 & 0 \\ 0 & 0 & 0 & 0 & q_{55}^2 \end{bmatrix} \tag{34}$$

If Q_v is too large, the Kalman gain will decrease, thus, the estimation fails to update the propagated disturbance based on measurement. In (33), σ_{γ_gyro} and σ_{c_GPS} denote the variance of yaw rate noise and course angle noise, respectively. They are chosen based on the idea that measurement of course angle is more reliable than measurement of yaw rate. Small Q_w results in unstable estimation. On the other hand, large Q_w forces the estimation to completely rely upon the measurements. Therefore, the noise associated with the measurement is directly transmitted into the estimated values.

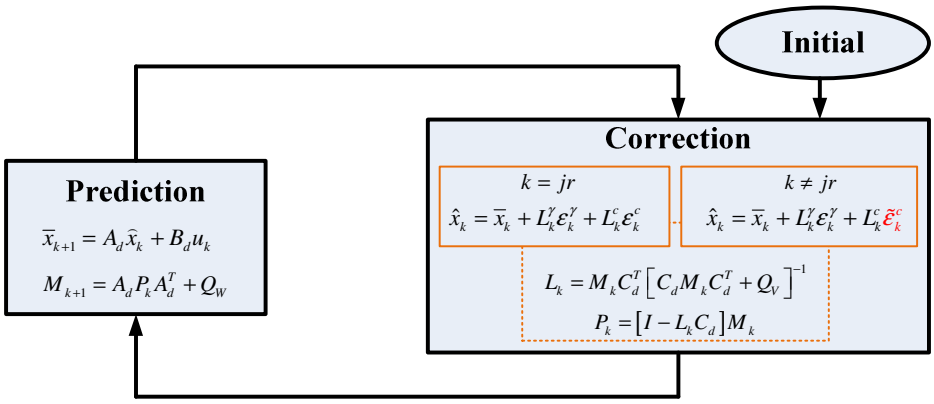

Fig. 5. Algorithm of sideslip angle estimation using multi-rate Kalman filter with prediction of course angle residual.

At step $k = jr$, both yaw rate and course angle are update, thus, estimated states are corrected with real course angle residual and real yaw rate residual:

$$\hat{x}_k = \bar{x}_k + L_k^{\gamma}\varepsilon_k^{\gamma} + L_k^{c}\varepsilon_k^{c} \tag{35}$$

At step $k = jr + 1$, only yaw rate is updated, thus, estimated states are corrected with real yaw rate residual and predictive course angle residual, using the prediction formula (20).

$$\hat{x}_k = \bar{x}_k + L_k^{\gamma}\varepsilon_k^{\gamma} + L_k^{c}\tilde{\varepsilon}_k^{c} \tag{36}$$

GPS INTERFACE DESIGN

GPS receiver CCA-600 outputs the information in NMEA-0183 protocol. In order to transfer data from CCA-600 to the experimental vehicle, GPS interface software is designed in a laptop (Fig. 6). It receives the NMEA messages from CCA-600 through serial port. Then, it decodes the messages for required data, such as vehicle position, course angle, and velocity. The decoded data are sent to the controller of experimental vehicle through LAN cable using user datagram protocol (UDP/IP). Measurements of course angle and velocity using the GPS interface are shown in Fig. 7.

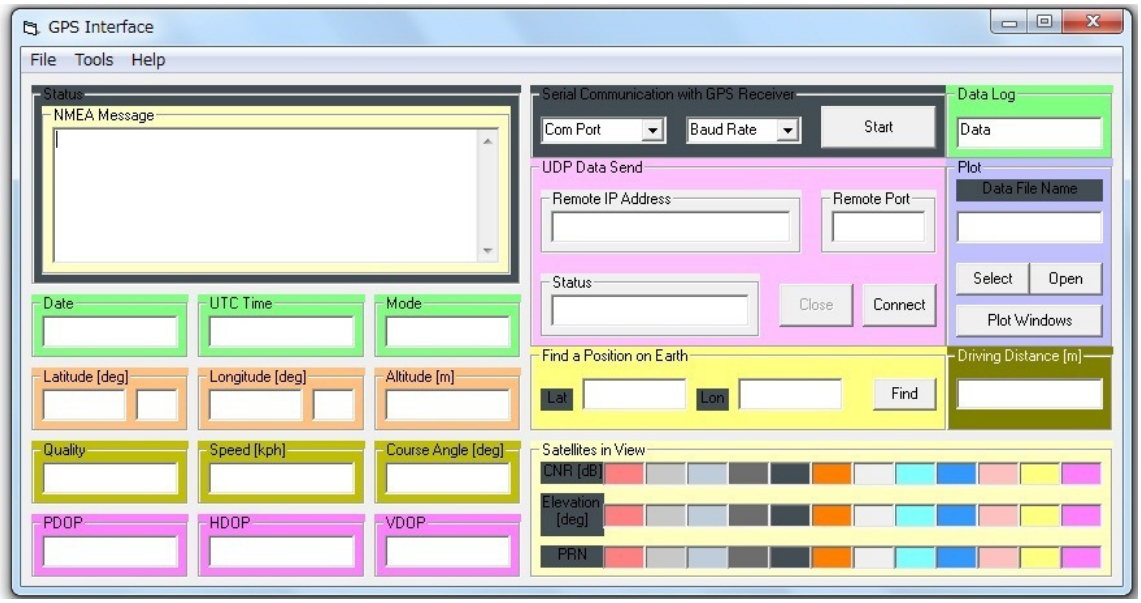

Fig. 6. GPS interface software.

(a) (b)

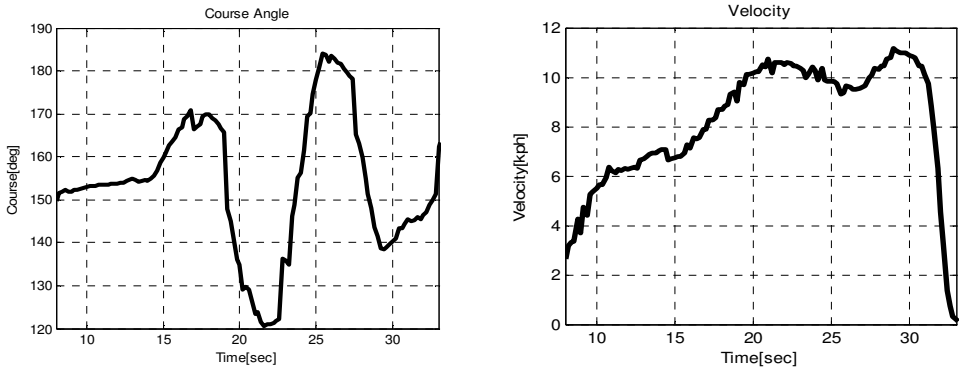

(c) (d)

Fig. 7. Data recorded by GPS interface:
(a) Vehicle position on Google Earth, (b) Experiment place, (c) Course angle, (d) Velocity

EXPERIMENT RESULTS

In order to demonstrate the effectiveness of the proposed method, other three sideslip angle estimation methods are performed. The proposed method is named "Enhanced Three-State MRKF" in this study. The name and description of each method are listed as follows:

- Two-State KF: The single-rate Kalman filter using only yaw rate measurement.
- Three-State MRKF: Conventional multi-rate Kalman filter using yaw rate and course angle measurement. During inter-samples, sideslip angle is corrected based on yaw rate residual only.
- Three-State MROb: From literature review, the enhancement of inter-sample estimation was proposed by Hara *et al* [8]. The key idea of this method is to hold the real residual to correct the estimated state during inter-samples. The observer gain is redesigned to confirm the convergence and stability of estimation. This method was applied in hard disk drive system. We re-apply this method for sideslip angle estimation by holding the real course angle residual during inter-samples. It is important to notice that, the multi-rate ratio in case of hard-disk drive ($r < 10$) is smaller than the multi-rate ratio of vehicle system, due to the limitation of GPS receiver ($r = 200$ in this study). Moreover, vehicle control system is a time varying system due to the change of road friction coefficient and velocity. The unknown external disturbance may be introduced into the system. Therefore, in case of vehicle system, Kalman filter is applied because it is the optimal linear estimator in sense that no other linear filter can gives a smaller variance of estimation error.

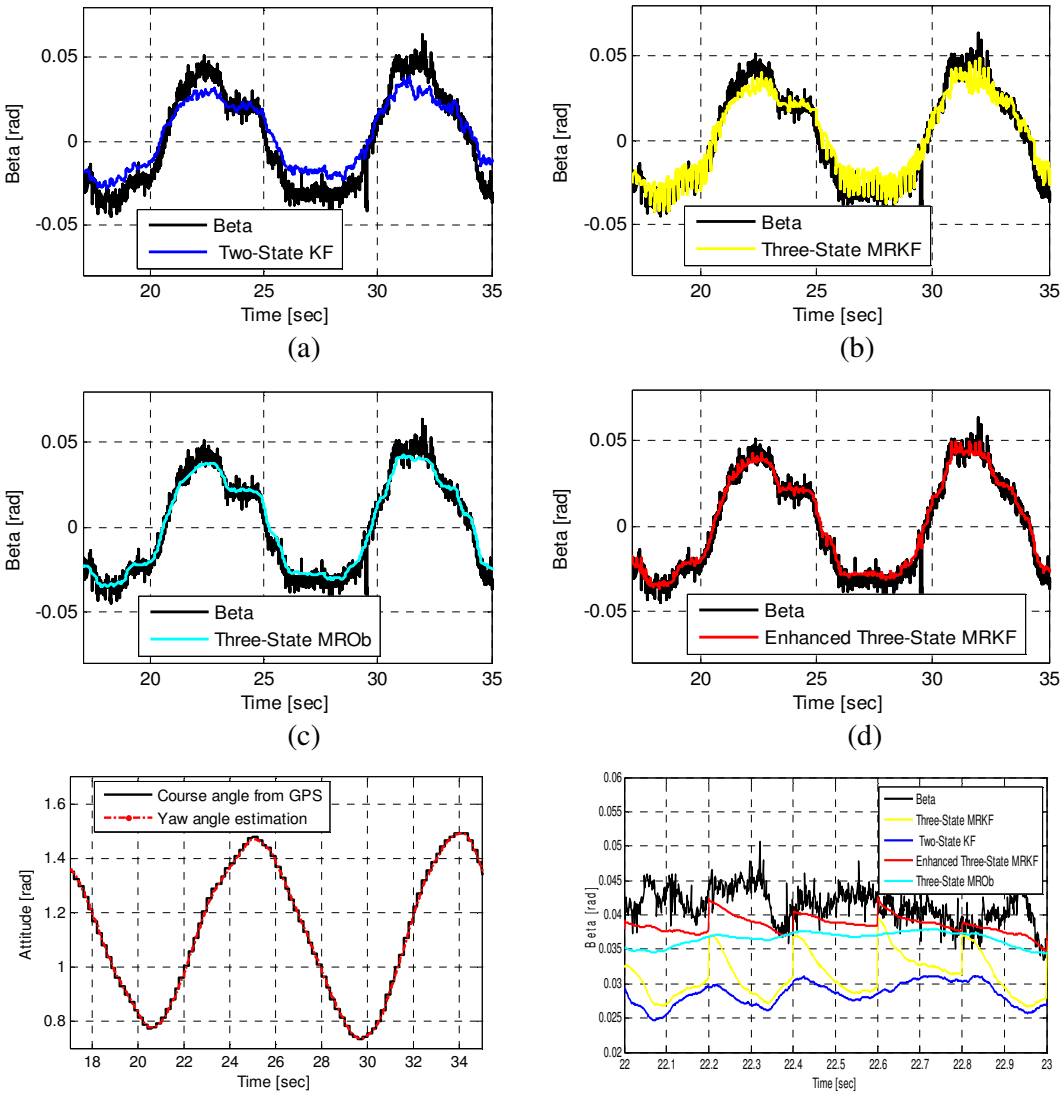

Fig. 8. Lane change test experiment results
(a) Two-state KF, (b) Three-State MRKF , (c) Three-State MRObs,
(d) Enhanced Three-State MRKF, (e) Vehicle attitude, (f) Inter-sample performance

Fig. 8 shows the results of lane-change test on the asphalt road surface. The real cornering stiffness are C_f= 10,000 [N/rad] and C_r = 10,000 [N/rad]. However, the cornering stiffness of the estimation model are set as C_{fm} = 7000 [N/rad] and C_{rm} = 7000 [N/rad]. This makes the model error condition for experiment. Two-State KF shows the poorest estimation performance. Three-State MRKF shows the better estimation result. The estimation error is reduced when course angle is updated. However, during inter-samples, sideslip angle is corrected by only yaw rate measurement, the estimation performance of Three-State MRKF is degraded. From Fig. 8 (f), thanks to the prediction of course angle residual, Enhanced Three-State MRKF shows the best estimation performance. Besides sideslip angle estimation, yaw angle is estimated at 1 kHz in comparison with 5 Hz course angle, as shown in Fig. 8 (e). Root-mean-square-deviation (RMSD) from measured sideslip angle is calculated for

comparison. The results is shown in Table 2 in which, the proposed method has the smallest RMSD value.

TABLE 2
RMSD OF SIDESLIP ANGLE ESTIMATION

Estimation method	RMSD [rad]
Two-state KF	1.02×10^{-2}
Three-state MRKF	0.86×10^{-2}
Three-state MROb	0.48×10^{-2}
Enhanced three-state MRKF	0.36×10^{-2}

CONCLUSIONS

From the view of control theory, this paper proposes a new method for enhancing the multi-rate estimation. During inter-samples, estimated state is corrected with the predictive measurement residual. The proposed method is applied in sideslip angle using GPS and multi-rate Kalman filter for vehicle control system. Experiments are conduct to evaluate the effectiveness of the proposal in comparison with the previous estimation methods. Even under model error, accurate sideslip angle estimation is achieved. In future works, auto-tuning of process noise and measurement noise covariance matrix will be examined.

ACKNOWLEDGEMENT

The authors would like to thank Japan Radio Company (JRC) for their supports of GPS receiver for experiments in this study.

REFERENCES

[1] J. Y. Wong. Theory of Ground Vehicles. John Wiley & Sons, INC, Third Edition, 2001.
[2] Corrsys-Datron: http://www.corrsys-datron.com/optical_sensor.htm
[3] C. Geng, L. Mostefai, M. Denai, and Y. Hori. Direct Yaw Moment Control of an In Wheel Motored Electric Vehicle Based on Body Slip Angle Fuzzy Observer. IEEE Transactions on Industrial Electronics, Vol. 56, pp. 1411-1419, 2009.
[4] Y. Wang, B. M. Nguyen, P. Kotchapansompote, H. Fujimoto, and Y. Hori. Vision-based Vehicle Body Slip Angle Estimation with Multi-rate Kalman Filter Considering Time Delay. 21st IEEE International Symposium on Industrial Electronics, 2012.
[5] D. M. Bevly, J. Ryu, and J. C. Gerdes. Integrating INS Sensors with GPS Measurements for Continuous Estimation of Vehicle Sideslip, Roll, and Tire Cornering Stiffness. IEEE Transactions on Intelligent Transportation System. Vol. 7, No. 4, pp. 483-493, 2006.
[6] R. Anderson and D. M. Bevly. Estimation of Slip Angles Using A Model Based Estimator and GPS. American Control Conference 2004, pp. 2122-2127, 2004.
[7] K. Nam, S. Oh, H. Fujimoto, and Y. Hori. Vehicle State Estimation For Advanced Vehicle Motion Control Using Novel Lateral Tire Force Sensors. American Control Conference 2011, pp. 4853-4858, 2011.
[8] T. Hara and M. Tomizuka. Performance Enhancement of Multi-rate Controller for Hard Disk Drives. IEEE Transactions on Magnetics, Vol. 35, No. 2, pp. 898-903, 1999.